MODELING AN IODINE HALL THRUSTER PLUME IN THE IODINE SATELLITE (ISAT)

Maria Choi
NASA Glenn Research Center
Cleveland, OH

ABSTRACT

An iodine-operated 200-W Hall thruster plume has been simulated using a hybrid-PIC model to predict the spacecraft surface-plume interaction for spacecraft integration purposes. For validation of the model, the plasma potential, electron temperature, ion current flux, and ion number density of xenon propellant were compared with available measurement data at the nominal operating condition. To simulate iodine plasma, various collision cross sections were found and used in the model. While time-varying atomic iodine species (i.e., I, I^+, I^{2+}) information is provided by HPHall simulation at the discharge channel exit, the molecular iodine species (i.e., I_2, I_2^+) are introduced as Maxwellian particles at the channel exit. Simulation results show that xenon and iodine plasma plumes appear to be very similar under the assumptions of the model. Assuming a sticking coefficient of unity, iodine deposition rate is estimated.

INTRODUCTION

Hall-effect thrusters (HET) are relatively low-cost electric propulsion devices that can be utilized for a wide range of ambitious long-duration NASA missions. Xenon (Xe) is an attractive propellant because it does not chemically react with spacecraft surfaces, and has larger mass and ionization cross section compared to other inert gases, yielding higher thrust for a given input power (T/P). However, Xe is relatively expensive and must be stored in large high-pressure tanks [1]. Due to these limitations, a variety of alternatives have been proposed, and iodine has been identified as an attractive alternative propellant for HETs, especially for small satellites (<300kg) and exploration class missions [2]. Iodine is almost as heavy as, is easier to ionize than, and has about three times the storage density of Xe [3]. The feasibility of a Hall thruster operation using iodine propellant has been proven through experimental testing of Busek's 200-W Hall thruster (BHT-200), which yielded stability and performance comparable to that observed with Xe, higher thrust to power ratio at higher power operating condition, and lower beam divergence at certain operating conditions [3, 4].

Despite its advantages, using iodine as a propellant has one critical risk, which is associated with its high reactivity. Reactive atomic iodine (I) may potentially cause contamination or corrosion of spacecraft surfaces and solar arrays, which is a concern for spacecraft system integration. Since the majority of Hall thruster experiments that utilize iodine have focused on the thruster and subsystem performance, there is a dearth of detailed knowledge of physical processes occurring in the plume of the thruster and thus their effect on spacecraft surfaces. Moreover, due to the contribution from molecular iodine (I_2), many different types of reactions may occur in some regions—including dissociative ionization, electron attachment, and inelastic energy exchange—that are very different from the nature of Hall thrusters operated on Xe. Although there have been extensive experimental efforts in using iodine as a Hall thruster propellant, results from modeling work associated with the iodine thruster plume and its effect on spacecraft surfaces have not been published to date. Modeling the iodine plasma plume and its interaction with the spacecraft surfaces is necessary in order to further understand its use as a propellant and mitigate any potential harmful surface-plume interactions.

This study is concerned with numerical simulations of the iodine plasma plume generated by BHT-200 Hall thruster (shown in the left of Figure 1), which would be the first iodine-operated Hall thruster that will be flown in space in the Iodine Satellite (iSAT). The basic configuration of

iSAT, including the BHT-200 thruster and other components of the propulsion system are shown in the right of Figure 1, and more details about the iSAT mission can be found in Ref. [1]. Since the iodine plasma properties of the BHT-200 thruster plume have not been measured, the simulation is performed first using xenon as a propellant for a validation of the model. To simulate the iodine plasma plume, various collision cross sections were found and used in the hybrid PIC model, Draco. In a Hall thruster plume, iodine exists as both atomic (i.e., I, I^+, I^{2+}) and molecular (i.e., I_2, I_2^+) species. Due to these mixtures, complex physical processes may occur, and thus modeling an iodine plume can be challenging and requires some assumptions, which are discussed in the next section. Finally, the iodine particle flux on the spacecraft surface is found to estimate its deposition rate.

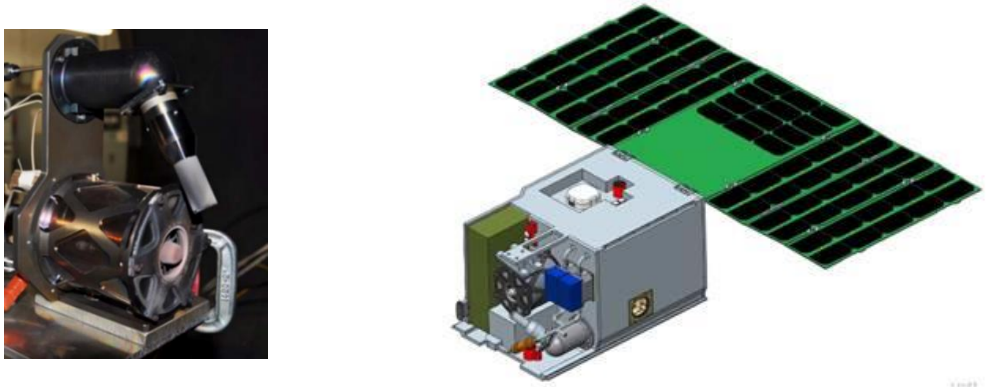

Figure 1. Left: Busek's 200 W Hall thruster (BHT-200). Right: Basic configuration of iSAT including the BHT-200 Hall thruster in the front and the solar arrays in the back of the satellite.

MODEL DESCRIPTIONS

The model employed in this study, Draco [5], is a software framework developed under COLISEUM framework by Air Force Research Laboratory (AFRL). Draco is a 3-D parallel hybrid code that was developed to study electric thruster plumes and their interaction with spacecraft components. In Draco, the surface is defined using a triangular mesh, while a Cartesian volume mesh is used for the Draco's computation domain. For an illustration of the surface and volume meshes used in this simulation, Figure 2 shows 1) the surface mesh of the iSAT spacecraft and the BHT-200 Hall thruster, created using Cubit, and 2) the rectilinear volume mesh generated by Volcar—Draco's built-in mesh generator—with a contour plot of the number density of Xe^+, on the left and right sides, respectively.

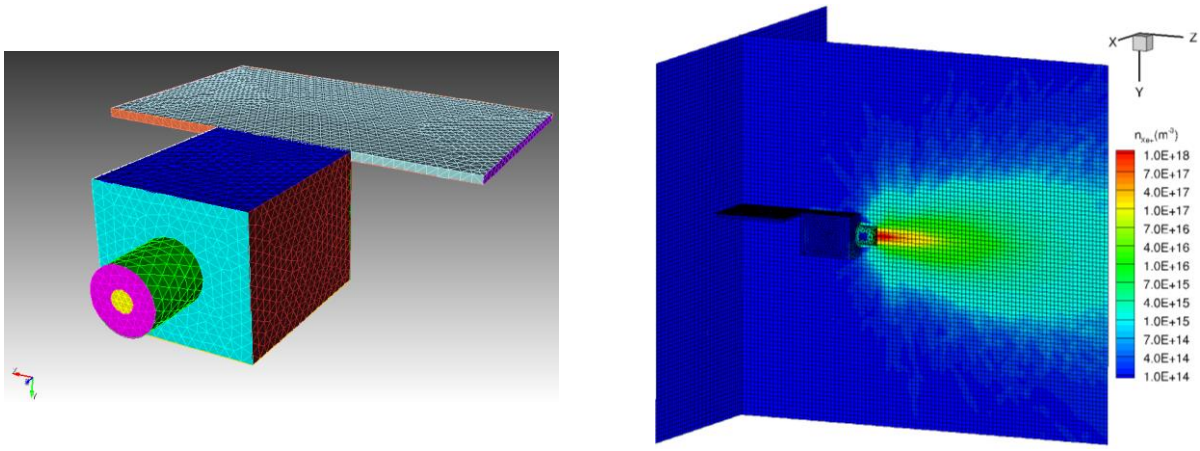

Figure 2. The geometry and surface mesh of the iSAT spacecraft and BHT-200 thruster, created using Cubit (left), and the cross-section view of the volume mesh with ion number density contour (right).

PLASMA DYNAMICS

In the current model, the transport of heavy species are simulated using the particle-in-cell method (PIC) [6] combined with either direct simulation Monte Carlo (DSMC) [7] or Monte Carlo Collision (MCC). The motions of charged particles in plasmas are governed by the Lorentz force $\boldsymbol{F}$:

$$\boldsymbol{F} = q(\boldsymbol{E} + \boldsymbol{v} \times \boldsymbol{B}) \tag{1}$$

where $\boldsymbol{E}$ is electric field, $\boldsymbol{B}$ is magnetic field, and $\boldsymbol{v}$ is particle velocity. In Hall thrusters, the magnetic field is not strong enough to affect the motion of ions.

In the PIC method, the charge density at each grid point is calculated from the distribution of particles in each cell. From the charge density, quasi-neutrality ($n_e \approx n_i$) is assumed, and the plasma potential is obtained by solving the Boltzmann relation that can be derived from electron momentum conservation equation assuming thermal equilibrium, constant electron temperature, and no magnetic fields:

$$\phi = \phi_r + \frac{k_B T_{e,r}}{e} \ln\left(\frac{n_e}{n_{e,r}}\right) \tag{2}$$

where ϕ is electrostatic potential, T_e is electron temperature, n_e is electron number density, and subscript r represents a reference value. Instead of assuming a constant temperature in the entire domain, a polytropic temperature model can be used to provide more accurate representation of the electron temperature field, which results in the following modified Boltzmann relation:

$$\phi = \phi_r + \frac{k_B T_{e,r}}{e}\left(\frac{\gamma}{\gamma - 1}\right)\left[\left(\frac{n_e}{n_{e,r}}\right)^{\gamma - 1} - 1\right] \tag{3}$$

where γ is specific heat ratio. The electric potential is used then to calculate the electrostatic field and force on the particle from $\boldsymbol{E} = -\nabla\phi$. Then, the particle positions and velocities are updated by integrating Eq. (1) at each time step.

COLLISION DYNAMICS

In a Hall thruster plume, the two most important collision mechanisms are the momentum-exchange (MEX) and the charge-exchange (CEX) collisions between the neutral and ion species. The current study employs the MCC method [6] to simulate both MEX and CEX collisions between neutral-ion pairs, and the variable hard-sphere (VHS) model [7] to simulate the MEX collision between neutral-neutral pairs. In the MCC method, a source particle collides with a target "cloud," instead of an individual target particle. A collision probability is given by Birdsall [6] as:

$$P = 1 - \exp(-n_n \sigma g \Delta t) \tag{4}$$

where n_n is the number density of target particles, σ is the collision cross section, and g is the relative velocity. If this probability is larger than a random number, a collision occurs and the type of collision is determined.

If a CEX collision occurs between an ion and a neutral cloud, the velocities of the collided ion are replaced with random values obtained by sampling the Maxwellian distribution at the neutral temperature. The Maxwellian distribution is given as:

$$f_M = \sqrt{\frac{2k_B T}{m}}\left(\sum_{i=1}^{M} R_i - \frac{M}{2}\right)\left(\frac{M}{12}\right)^{1/2} \tag{5}$$

where k_B is the Boltzmann constant, T is temperature, m is particle mass, R_i is a random number between 0 and 1, and M is the number of R_i.

To account for the strong forward-scattering tendency of fast ion and slow neutral collisions, scattering angles are calculated using a differential cross section. A fit to an experimental

CEX differential cross section measurement for xenon in a Hall thruster [11] is found and implemented by Scharfe [8].

CROSS SECTION MODELS

As shown in Eq. (4), a collision cross section is necessary to calculate a collision probability. For neutral-neutral collisions, the VHS cross section [7] is employed:

$$\sigma_{VHS}(Xe,Xe) = \frac{2.12 \times 10^{-18}}{g^{2\omega}}\ m^2 \quad \textbf{(6)}$$

where g is the relative velocity and $\omega = 0.12$ is related to the viscosity temperature exponent for xenon. For modeling CEX collisions, Hall thruster modeling community often uses the following semi-empirical form of cross sections:

$$\sigma_{CEX} = A - B\log(E) \quad \textbf{(7)}$$

where A and B are fitting parameters to experimental data and E is the collision energy in eV in the laboratory frame. For xenon collisions, the CEX collision cross sections between a Xe neutral and single- and double-charged Xe ions were measured by Miller *et. al.* [9], and the fitting coefficients to Miller's experimental data using Eq. (7) are summarized in Table 1.

Table 1. Coefficients in Eq. (7) for xenon and iodine CEX collision cross sections.

	A	B
Xe-Xe$^+$	87.3	13.6
Xe-Xe^{2+}	45.7	8.9
I_2-I$^+$	66.0	4.7

Modeling an iodine plasma plume can be more complicated than xenon because there are more reaction and collision types to account for due to the presence of molecular iodine species, i.e., I_2 and I_2^+. The likelihood of various collisions occurring depends on their collision cross sections. The present work does not attempt to solve all rate equations to determine which collisions are important to consider. Instead, just as in a xenon-operated Hall thruster plume, it is reasonable to assume that an efficient long-range CEX collision is important also in an iodine-operated Hall thruster plume, because the CEX collision produces slow ions and fast neutrals that affect the thrust performance and lifetime. Since iodine exists as in both atomic and molecular states in a Hall thruster plume, we need to consider the CEX collisions between all of the following cases: 1) atomic neutral and atomic ion (I-I^+), 2) molecular neutral and atomic ion (I_2-I^+), and 3) molecular neutral and molecular ion (I_2-I_2^+). Other species combination could be considered for more accurate collision modeling, but only these three types of collisions are considered in the current study. Recently, the CEX collision cross sections for I_2-I^+ and I_2-I_2^+ were measured by Hause *et. al.* [10]. The fitting coefficients to Eq. (7) are found for I_2-I^+, as $A = 66$ Å and $B = 4.7$ Å, as summarized in Table 1. Since a fit for I_2-I_2^+ data to Eq. (7) was not determined in Ref. [10], we determined an analytical fit to this CEX cross section data using the following form:

$$\sigma_{CEX}(I^+,I_2) = c_1\log^3(E) + c_2\log^2(E) + c_3\log^1(E) + c_4 \quad \textbf{(8)}$$

where c_1, c_2, c_3, and c_4 are fitting coefficients defined as in Table 2 below.

Table 2. Values of the fitting coefficients in Eq. (8).

c_1	c_2	c_3	c_4
-0.47	3.5	-9.0	82.0

Since a measurement of the cross section of I-I^+ is not available, a semi-empirical formula that relates the cross section with its ionization potential, ε_I, and impact velocity, v, by Sakabe and Izawa [11] is used to calculate the unknown cross section:

$$\sigma(v) = [A - B\ log_{10}(v)]\left(\frac{\varepsilon_I}{\varepsilon_{I_0}}\right)^{-1.5} \quad \textbf{(9)}$$

where $A = 1.81 \times 10^{-14}$, $B = 2.12 \times 10^{-15}$, and $\varepsilon_{I_0} = 13.6$ eV is the ionization potential of hydrogen. For iodine, the first ionization potential of atomic iodine was used (i.e., $\varepsilon_I = 10.5$ eV). In order to verify this cross section model, the cross section of xenon is calculated using Eq. (9) and is compared with Miller's cross section for xenon as shown in Figure 3. Sakabe's formula predicts Miller's cross section for xenon very well. Thus, the cross section for I- I^+ is found using Sakabe's formula and employed in current study. All CEX cross sections that are modeled in Draco are shown in Figure 4. The CEX cross section for I- I^+ is lower than Xe- Xe^+ for increasing impact energy, so fewer collisions are expected for I- I^+ than Xe- Xe^+. On the other hand, I_2- I_2^+ is higher than Xe- Xe^+ for increasing impact energy.

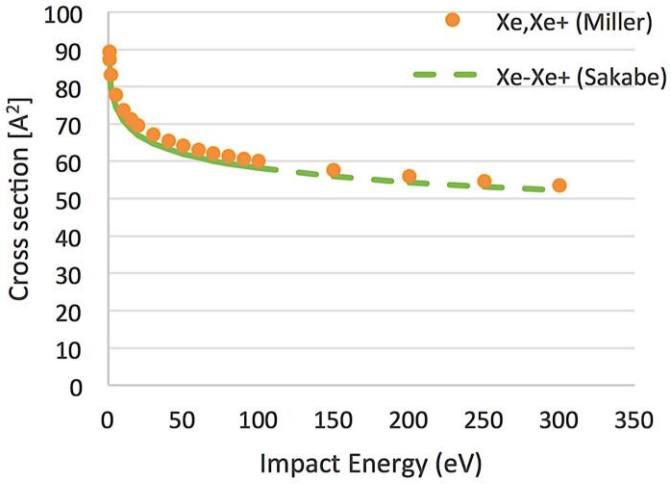

Figure 3. Charge-exchange collision cross section as a function of impact energy. Sakabe's formula predicts Miller's semi-empirical fit very well.

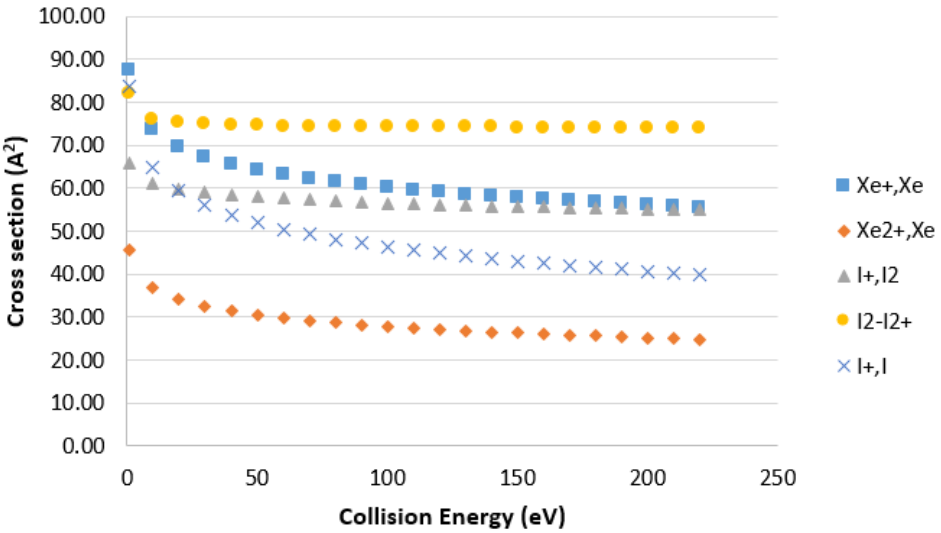

Figure 4. Charge-exchange collision cross sections for all species modeled.

KEY ASSUMPTIONS USED IN MODELING IODINE PLASMA PLUME

Performing a plasma plume simulation using Draco requires neutral and ion particle information at the thruster exit as an input condition. The effect of input source types in Draco have been studied before [12, 13]. Among other source options, utilizing HPHall Spawn to provide the particle information to the plume was proven to be the most effective option. Thus, we simultaneously run HPHall [14] to model the Hall thruster discharge plasma and to provide an accurate time-dependent particle information to Draco at each time step. Figure 5 shows the simulation domain of HPHall, with a contour plot of an electron number density. HPHall sends the particle information to Draco along a user-defined lambda line (not shown).

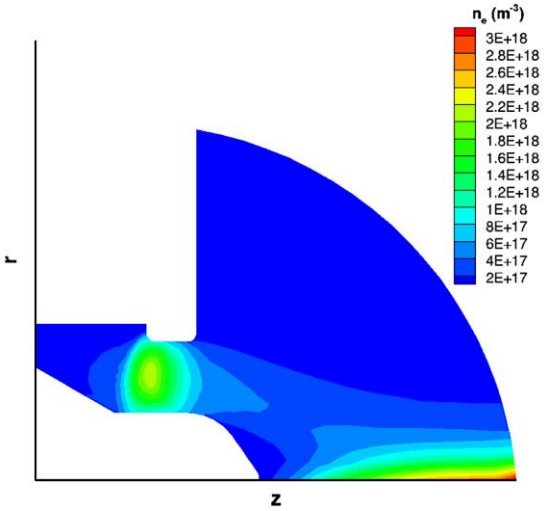

Figure 5. Contour plot of electron number density from HPHall simulation, ran simultaneously to provide detailed input to Draco.

Due to the mixture of atomic and molecular iodine species, a number of reactions involving I_2 may occur in the thruster and the plume, including dissociation, ionization, electron attachment, inelastic energy exchanges (e.g., rotational and vibrational), and recombination. Especially, since I_2 has a low dissociation energy threshold (1.54 eV) and a large ionization cross section (peak cross section = 12.3 A^2), a dissociative ionization process is likely to occur in the ionization region of the discharge channel. This process should be modeled in HPHall for a physically accurate model of the iodine plume. Since HPHall currently models only the neutral atom, singly- and doubly-charged ions, implementing additional reactions in HPHall involves modifying significant portion of HPHall. More importantly, a detailed reaction modeling is not the focus for this work. Rather, the goal is to provide a first-order approximation of the iodine particle flux on spacecraft surfaces using the numerical tools available to us at this stage.

For the iodine plume simulation, only I, I^+, and I^{2+} species are simulated in HPHall, and I_2 and I_2^+ are injected as separate inflow species at the thruster exit plane assuming Maxwellian velocity distributions, resulting in all five iodine species (I, I^+, I^{2+}, I_2, and I_2^+) handled by Draco in the plume. The mass flow rate of I_2^+ has been estimated based on measured mole fraction data shown in Table 3, and the mass flow rate of I_2 is assumed to be 10% of the total neutral flow rate, which is calculated from the mass utilization efficiency of 85.3% [3].

All simulations are performed at the nominal operating condition of the BHT-200 thruster, as shown in Table 4, with the background neutral number density equivalent to the vacuum chamber pressure of 5×10^{-6} Torr. The MEX and CEX collisions are ignored in HPHall simulations but included in the plume simulation using Draco. The mass and ionization cross section for each species was appropriately incorporated in HPHall.

Table 3. Xenon and iodine ion species distributions in the BHT-200 Hall thruster plume [3].

Species	Mole Fraction, Xe	Mole Fraction, I
I_2^+		0.029
Xe^+, I^+	0.975	0.953
Xe^{2+}, I^{2+}	0.021	0.015
Xe^{3+}, I^{3+}	0.004	0.003

Table 4. Summary of nominal operating conditions for the BHT-200 Hall thruster.

	Xenon [12]	Iodine [3]
Discharge voltage (V)	250	250
Discharge current (A)	0.75	0.74
Anode mass flow rate (mg/s)	0.84	0.82
Cathode mass flow rate (mg/s)	0.098	0.096
Mass (propellant) utilization efficiency	0.981	0.853

RESULTS AND DISCUSSION

As a model validation, the first comparison is made between the simulation results and the laboratory measurements of xenon plume plasma parameters of the BHT-200 thruster from Ref. [12]. The left side of Figure 6 shows angular profiles of the plasma potential at a radius of 10 cm away from the thruster exit plane, compared with experimental data. The simulated plasma potential value shows an excellent agreement with the experimental data, where both results monotonically decrease from 19 V to 2.0 V, from 0 degree to 90 degrees. The right side of Figure 6 compares the angular profiles of the simulated and measured electron temperature at 10 cm away from the thruster exit plane. The electron temperature predicted by the model decreases from 3.8 eV to 0.94 eV from 0 to 90 degrees, while the measured data decreases from 2.6 eV to 0.36 eV. Despite the over-estimation of Te by 1 eV, the overall trend agrees well with the measured data. The small discrepancy in the magnitude of the electron temperature is likely due to the limitation of the polytropic temperature law and/or the choice of the reference values for the Boltzmann relation.

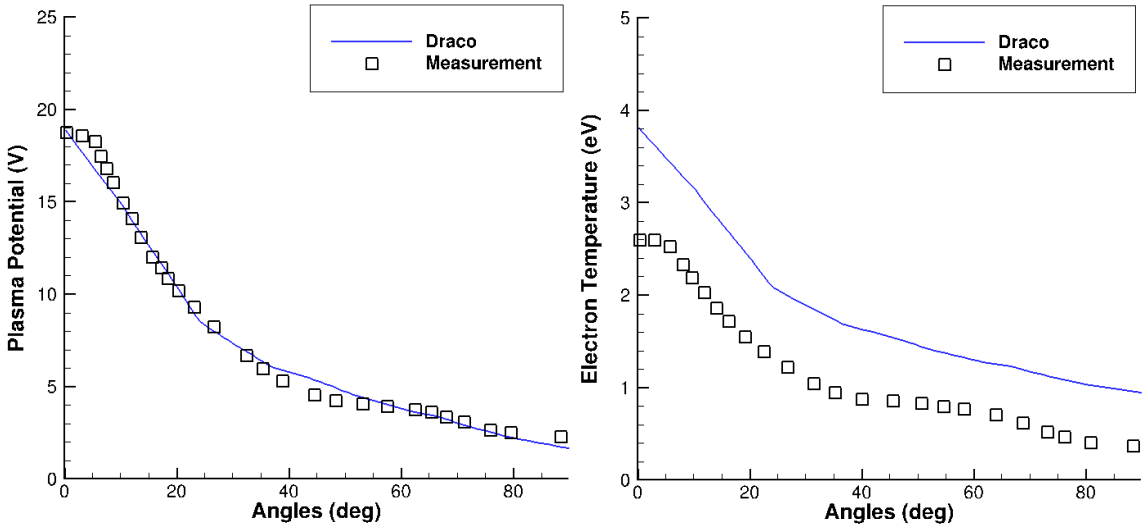

Figure 6. Angular profile of the plasma potential (left) and electron temperature (right) at a radius of 10 cm away from the centerline of the thruster exit plane.

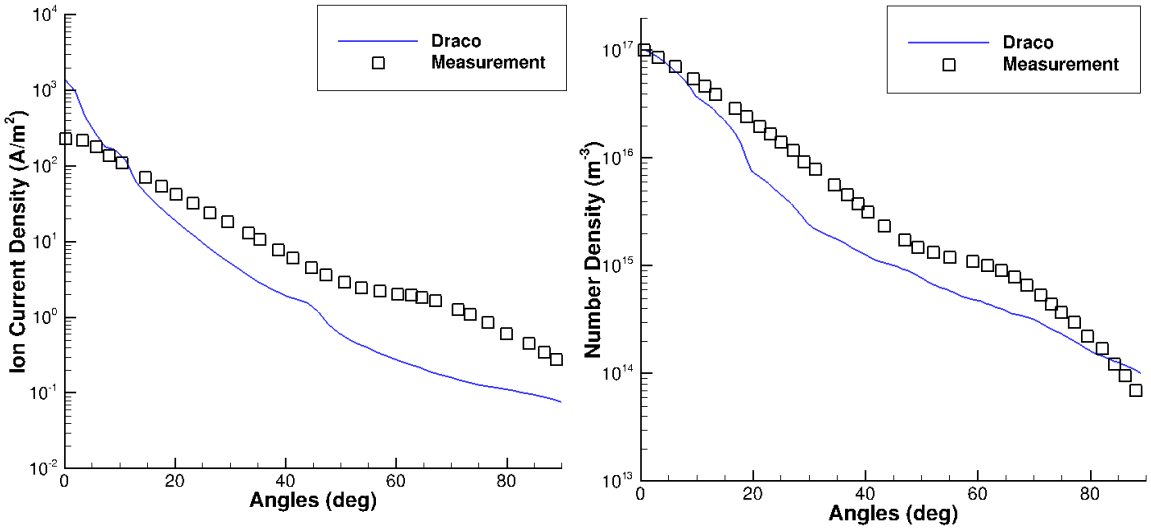

Figure 7. Angular profile of the ion current density from an RPA probe (left) and the ion number density (right) at a radius of 10 cm away from the centerline of the thruster exit plane.

The left side of Figure 7 shows the numerical angular RPA trace, compared with the collected ion current density by an RPA probe. The ion current density is over-estimated near the thruster centerline (< 5 deg.) and is under-estimated at larger angles (> 20 deg.), especially around 60-70 degrees where the charge-exchange wing is observed from the measurement. The comparison shows that the model predicts a more collimated plume than the measurement at this operating condition. The right side of Figure 7 compares the ion number density predicted by the model with experimental data. While the model provides reasonably good magnitudes in general, the overall shape is not well captured. Although the discrepancies in ion properties could be minimized by using better choices of the reference values for the Boltzmann relation in Draco and anomalous mobility parameters in HPHall, it was decided that the model provides a reasonable agreement with experimental data overall for the purpose of this work, which is to estimate the flux of iodine on the spacecraft surfaces.

Next, we compare the xenon plume simulation results with the iodine. In Figure 8, number densities of the total neutral and ion species are compared on the left and the right, respectively. From the qualitative comparison, both Xe and I show similar contours of the neutral and ion number densities overall. Xe and I have similar mass and ionization potential, and there are very few molecular iodine species in the plume. The sum of the molecular species (not shown) have at least an order of magnitude smaller current and number densities than the singly-charged atomic iodine ion (I^+). Similar observation is made in the plasma potential and ion current density for Xe and I in Figure 9. These results are not surprising because similar performance and plume efficiencies between Xe and I were measured at this operating condition before [4]. Moreover, the mass flow rates of the molecular species were based on experimental data.

The contour plots of the total neutral and ion particle fluxes on the surface of the iSAT satellite are shown in Figure 10. The fluxes of both neutrals (I and I_2) and the ions (I^+, I^{2+} and I_2^+) on the surface of the iSAT decrease away from the thruster exit channel because the neutral number density in the plume decreases as $1/r^2$, where r is the distance from the thruster exit. However, the fluxes appear to be slightly higher towards the outer edges of the front surface of the iSAT body than the inner region. Moreover, the front of the solar array shows the most amount of particle fluxes. The highest neutral and ion fluxes on the entire spacecraft are observed on the front pole pieces of the thruster. Due to the low density of neutral particles, the surface flux contour appears to be coarse, which would improve with increased run-time.

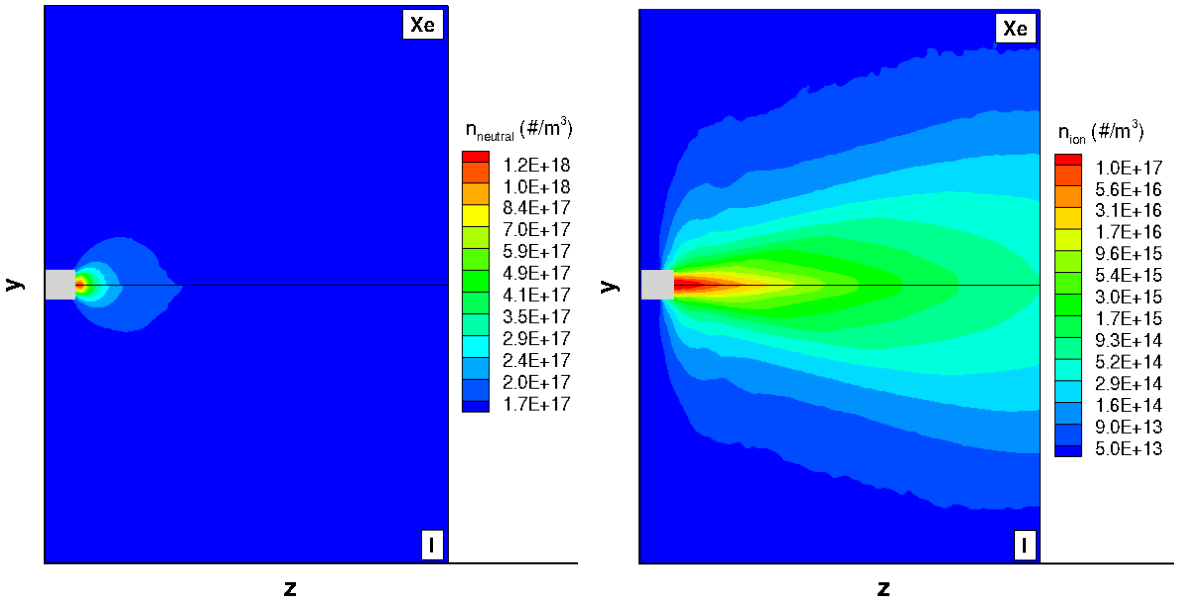

Figure 8. Comparison of total neutral (left) and ion (right) number densities of xenon (Xe) and iodine (I) species.

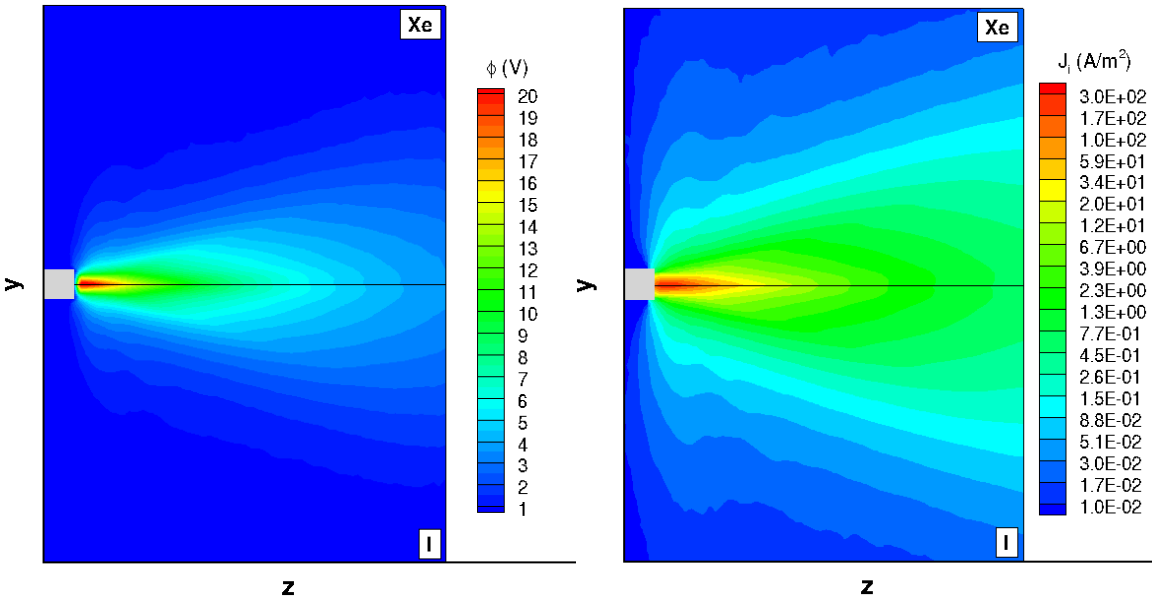

Figure 9. Comparison of the plasma potential (left) and total ion current density (right) of xenon (Xe) and iodine (I) species.

Based on these results, the highest neutral and ion particle fluxes on the solar array are calculated as approximately 3.5×10^{16} $m^{-2}s^{-1}$ and 1.0×10^{16} $m^{-2}s^{-1}$, respectively. Assuming 100% of the total incident particles sticks to the surface of the solar array and a constant rate of deposition, which is an extremely high conservative estimate, the deposition rate of iodine particles on the solar array would be approximately 0.007 μm/hr, which translates to the deposition per unit of approximately 0.34 mg/cm^2 over the entire thruster operation duration (~10 hrs).

However, not all iodine particles hitting the solar panel surface will deposit or chemically react to the surface, given high vapor pressure of iodine at the temperature of the solar panel. The portion of particles that actually react to the surface will depend on the surface properties of the solar panel, which is beyond the scope of this work. Moreover, the incident iodine flux on the

thruster surface is almost an order of magnitude higher than the flux on the spacecraft body or solar array, which could be a concern in the future for much longer thruster operation duration than the iSAT mission.

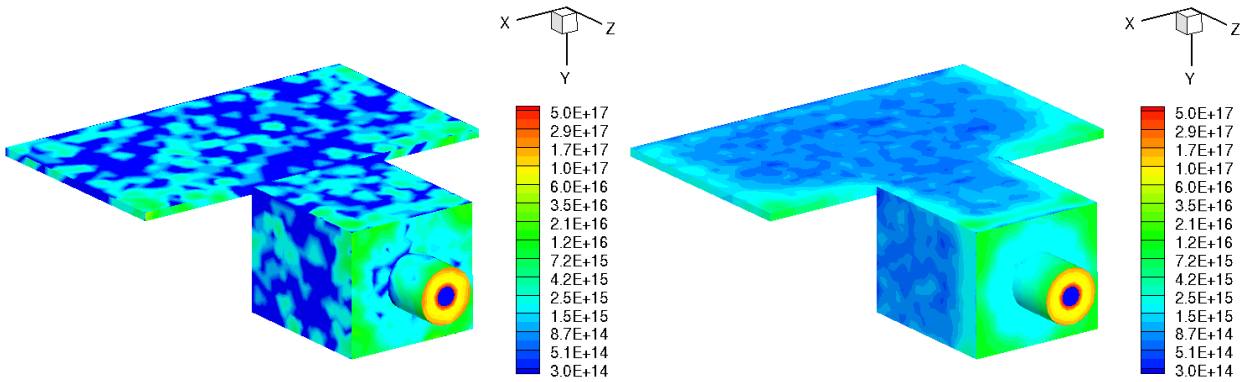

Figure 10. Contours of the total neutral (left) and ion (right) particle fluxes of iodine on the iSAT surface in particles/(m^{2}s).

SUMMARY AND CONCLUSIONS

In this study, both xenon- and iodine-operated BHT-200 Hall thruster plumes were simulated using Draco to estimate the incident particle flux on the spacecraft surface of the iSAT satellite. The model was first validated using traditional Xe propellant by comparing with available data. Then, the iodine propellant—including I, I^+, I^{2+}, I_2, and I_2^+ species—was simulated using the collision cross sections found from literature. The atomic iodine species (I, I^+, and I^{2+}) were simulated using the HPHall to pass the particle information from the discharge channel to the plume, while the molecular species (I_2, and I_2^+) were introduced at the discharge channel exit assuming Maxwellian velocity distribution functions. Under these assumptions, the iodine simulation results looked very similar to xenon, likely because of the similar mass and ionization cross section, and low molecular species density in the plume.

Not all iodine particles hitting the solar panel surface will deposit or chemically react to the surface, given high vapor pressure of iodine at the temperature of the solar panel. However, the sticking coefficient was assumed to be unity as a highly conservative estimate. Based on this assumption, the highest total iodine flux on the solar array was calculated as approximately 4.5×10^{16} m^{-2}s^{-1}, which means the deposition per unit area would be approximately 0.34 mg/cm^2 over the entire thruster operation duration. In reality, only some portion of iodine colliding with the surface may chemically react with the surface, which could reduce the efficiency and/or performance of the solar panel. How many particles actually react to or reflect off the surface will depend on the surface properties of the solar panel, which is beyond the scope of this work. Finally, for more physically accurate simulation of iodine plasma plume, one needs to model the detailed reactions discussed in this paper, especially the dissociative ionization, inside the discharge channel.

ACKNOWLEDGMENTS

The author would like to thank John Yim and Gabriel Benavides for discussions on this work, and acknowledge that resources supporting this work were provided by the NASA High-End Computing (HEC) Program through the NASA Advanced Supercomputing (NAS) Division at Ames Research Center.

REFERENCES

[1] J. W. Dankanich, K. Polzin, D. Calvert and H. Kamhawi, "The iodine Satellite (iSAT) Hall Thruster Demonstration Mission Concept and Development," in *50th AIAA/ASME/SAE/ASEE Joint Propulsion Conference*, Cleveland, OH, July 28-30, 2014.

[2] J. Szabo, M. Robin, S. Paintal, B. Pote, V. Hruby and C. Freeman, "Iodine Plasma Propulsion Test Results at 1–10 kW," *Plasma Science, IEEE Transactions,* vol. 43, no. 1, pp. 141-148, 2015.

[3] J. Szabo, B. Pote, S. Paintal, M. Robin, A. Hillier, R. D. Branam and H. R. E., "Performance evaluation of an iodine-vapor Hall thruster," *Journal of Propulsion and Power,* vol. 28, no. 4, pp. 848-857, 2012.

[4] A. Hillier, *Revolutioning Space Propulsion Through the Characterization of Iodine as Fuel for Hall-Effect Thrusters,* Wright-Patterson Air Force Base, OH: M.S. Thesis, Air Force Institute of Technology, 2011.

[5] L. Brieda, R. Kafafy, J. Pierru and J. Wang, "Development of the DRACO Code for Modeling Electric Propulsion Plume Interactions," in *40th AIAA/ASME/SAE/ASEE Joint Propulsion Conference and Exhibit*, Fort Lauderdale, Florida, 12-14 July, 2004.

[6] C. K. Birdsall and A. B. Langdon, Plasma physics via computer simulation, Philadelphia and New York: CRC Press, 2004.

[7] G. A. Bird, Molecular Gas Dynamics and the Direct Simulation of Gas Flows, Oxford: Oxford University Press, 1994.

[8] M. K. Scharfe, J. Koo and G. Azarnia, "DSMC Implementation of Experimentally-Based Xe+ + Xe Differential Cross Sections for Electric Propulsion Modeling," No. AFRL-RZ-ED-TP-2010-275, AIR FORCE RESEARCH LAB EDWARDS, AFB CA PROPULSION DIRECTORATE, 2010.

[9] J. S. Miller, S. H. Pullins, D. J. Levandier, Y.-H. Chiu and R. A. Dressler, "Xenon charge exchange cross sections for electrostatic thruster models," *Journal of Applied Physics,* vol. 91, no. 3, p. 984, 2002.

[10] M. L. Hause, B. D. Prince and R. J. Bemish, "A guided-ion beam study of the collisions and reactions of I+ and I2+ with I2," *The Journal of Chemical Physics,* vol. 142, no. 7, 2015.

[11] S. Sakabe and Y. Izawa, "Simple formula for the cross sections of resonant charge transfer between atoms and their positive ions at low impact velocity," *Physical Review A,* vol. 45, no. 3, p. 2086, 1 February 1992.

[12] M. R. Nakles, L. Brieda, G. D. Reed, W. A. Hargus and R. L. Spicer, "Experimental and Numerical Examination of the BHT-200 Hall Thruster Plume," in *43rd AIAA/ASME/SAE/ASEE Joint Propulsion Conference & Exhibit, AIAA 2007-5305*, Cincinnati, OH, 8-11 July, 2007.

[13] R. L. Spicer, *Validation of the DRACO Particle-in-Cell Code using Busek 200W Hall Thruster Experimental Data,* Blacksburg, VA: M.S. Thesis i Aerospace Engineering, Virginia Polytechnic Institute and State University, 2007.

[14] J. M. Fife, *Hybrid-PIC Modeling and Electrostatic Probe Survey of Hall Thrusters,* Massachusetts Institute of Technology: Ph.D. Thesis, Department of Eronautics and Astronautics, 1998.